Eurographics Workshop on Graphics for Digital Fabrication (2016)
A. Medeiros e Sá, N. Pietroni, and K. Rodriguez Echavarria (Editors)

Restoration of Architectural Ornament for Historic Buildings

Karina Rodriguez Echavarria[1], Ran Song[1], Dean Few[1] and Asla Medeiros e Sá[†2]

[1] Cultural Informatics Research Group, University of Brighton, UK
[2] FGV EMAp & School for Applied Mathematics at FGV, Brazil

Abstract

Many geographic areas within cities and towns across the world display historic buildings with stylised architectural elements displaying the influences of periods and cultures throughout their history. Ornamental mouldings are architectural elements which are commonly found both in façades and the indoors of historic buildings. These mouldings support the embellishment of a building; however, its proper maintenance can be expensive. This is because, until now, the restoration and conservation of ornamental mouldings has been mainly a manual artisan activity. This research explores the introduction of digital fabrication technologies into this process. Digital Fabrication technologies, including graphic algorithms and additive manufacturing technologies, enable the design and fabrication of customisable ornamental mouldings. Hence, this paper proposes the definition and testing of a graphical workflow for the fabrication of ornamental mouldings. The restoration and conservation of historic buildings is a major economic sector in Europe. Hence, this paper contributes towards lowering their maintenance cost and making more accessible the ornamentation of new buildings.

Categories and Subject Descriptors (according to ACM CCS): I.3.8 [Computer Graphics]: Applications—I.4.6 [Computer Graphics]: Segmentation—J.5 [Computer Applications]: Arts and Humanities—Architecture

1. Introduction

After the rapid expansion of modern architecture in Europe, there was an enormous surge of interest in architectural heritage conservation towards the end of the 20th century. This led to the increasing demand to restore and retain in use historic buildings. Nevertheless, restoration of architectural historic forms requires knowledge of the original design and fabrication techniques [CL05]. These techniques have remained an artisan and manual activity, where methods developed hundreds of years ago are still used to maintain, repair, restore and extend building and their architectural elements. Where new technologies are used to mass produce these elements, they usually remain simple in shape and form as customisation is not yet possible.

Digital Fabrication technologies offer opportunities to support the cost-effective, customisable and on-demand fabrication of architectural forms. In this research, we focus mainly on architectural elements, particularly on ornamental mouldings, as they are usually referred as, to decorate interiors and exterior of buildings. These mouldings include coving/cornicing, ceiling roses, corbels, dados or panelling, pilaster and arches.

This paper presents research conducted towards defining and testing a graphical workflow to restore architectural ornamental mouldings using digital fabrication technologies. The paper is structured as follows. Section 2 presents background knowledge on the restoration of architectural ornament, while Section 3 discusses previous work. Section 4 presents two different algorithms to support the workflow. Section 5 presents a case study where the workflow is tested. Finally, Section 6 presents conclusions and further work.

2. Restoration of Ornamental Architectural Mouldings

Meyer [Mey74] defines the term decoration as the art of applying ornament to beautify objects. The style of decoration is usually determined by the aim and material of the object to be decorated and, secondly, by the ideas ruling at different periods and among different nations. Phillips and Bunce [PB93] trace patterns used in ornament from ancient and classical times through to the Gothic and Victorian periods, and culminating in the high-tech computer-aided designs we use today. Jones [Jon86] presents a comprehensive history of ornament along different periods and nations from antiquity to the medieval and the Renaissance in Europe, India, China, Pacific islands and the Islamic world.

In architecture, ornamental mouldings are typically used to embellish architectural elements in the interior or the exterior of a building creating a different style to the room or the façade that they decorate. Mouldings usually display a repeating *pattern*, which is defined as a design composed of one or more motifs, arranged in

† supported by CAPES Brazil

DOI: 10.2312/gdf.20161077

an orderly sequence [PB93]. The number of potential patterns and motifs which can be produced for any moulding is only bounded by the skills and tools available for producing the moulding.

Current practices to produce ornamental mouldings using plaster material involve either running or casting the plaster using a mould. Running requires of a wooden running mould with a sharp zinc profile. This mould is then pushed through the plaster along its length to create the moulding. Casting is a more complex process, as it requires of a mould in which plaster can be poured and retrieved when it has solidified. The moulding's template was traditionally carved in wood; hence, any modification requires producing another template. As a result of these production constraints, producing ornamental mouldings can become a lengthy and expensive process. Hence, current mouldings options available to the mass market are limited in the diversity of patterns and motifs. This is because customisation is not yet economically advantageous in particular for those elements that need to be casted.

Technologies such as CNC are increasingly being introduced into the process by milling the pattern to MDF, wood and foam. Once the CNC machine produces the moulding with a specific pattern a mould or negative can be manufactured. Moulds are produced using resin or rubber which is poured over the pattern to create an exact impression. Marshall [Mar07] reported his experience in collaborating with an ornamental plaster company to experiment with rapid prototyping. This made clear that issues such as knowledge exchange and trust are critical to support this traditionalist industry.

Figure 1: *Ornamental moulding in need of restoration in the interior of a household; top left) initial state of the ceiling; top right) ceiling after restoration with no ornament; bottom) restored area before gluing the ornaments to the ceiling and painting them*

Furthermore, when an ornamental moulding in a buildings needs to be restored, for instance, in a room within a household (see Figure 1); the process is mainly manual. It involves identifying a section of the moulding onsite and peeling the layers of paints from the moulding. Thereafter, an imprint is taken from the moulding to create a new mould. When more than one moulding is used, there is a manual process to identify each moulding type. The existing workflow restricts how much the shape can be repaired and brought back to its original condition. In this research we investigate the advantages of the conversion of this manual process into a digital workflow in which mouldings can be fabricated to match the existing ornament.

We assume that an existing part of the moulding might still be installed on site or that we have access to the original mouldings in a database of 3D ornament, such as the one described in [RES15]. Hence, the proposed digital workflow is as follows:

1. Digitise on-site ornamental mouldings;
2. Segment and produce watertight 3D meshes for the ornamental mouldings;
3. Digitally restore the ornamental mouldings to their original condition (if required);
4. Use digital fabrication techniques to manufacture and post-process the mouldings;
5. Incorporate the ornamental mouldings on-site.

The processes require user intervention at several stages, including the digitisation as well as the manufacturing stage. Nevertheless, automation on some stages of the process can be implemented through graphics algorithms.

3. Related Work

Cultural heritage organisations are becoming aware of the potential of digital fabrication technologies for restoration and conservation purposes. In [SCP*15], the authors describe the state-of-the-art with digital fabrication technologies for cultural heritage. The survey demonstrates how 3D technologies are increasingly being incorporated into heritage processes, including producing replicas, developing customised packaging, and supporting restoration. The survey also highlights problems in the digital fabrication workflow, such as the safety of 3D printed materials, the limitation of the printer's size, the accuracy of the reproduced colour and the quality of the output.

Restoration of an existing pattern is a different problem from synthesizing or modeling a pattern. Modeling or synthesizing from example is being explored in the graphics community, for instance, in [ZJL14] the authors propose a method to automatically synthesize a decorative pattern for digital fabrication. In the restoration context an exact replica of the available pattern is to be replicated, thus, digitisation is a more reliable approach then modeling or synthesizing by example. Digitisation is so far a consumer technology and we use a scanner and its usual post-processing steps in order to acquire a digital replica of a given ornamental mould.

One core technique to approach our problem is to automate the detection and segmentation of a motif out of a large 3D mesh. This problem was first raised in the computer vision community more than a decade ago. Some popular low-level image processing techniques such as wavelet-based spectral domain analysis [HLL01], Hough transform-based method [TTVG03] and image-based autocorrelation [LCT04] have been employed for extracting 2D patterns with structural and/or textural regularity from images. Recently, this topic has been extensively explored in the computer graphics community. Liu et al. [LMLR07] developed a semi-automatic method to segment periodic reliefs on triangle meshes where users were required to manually input anchor points for assisting the system to coarsely locate periodic reliefs. Pauly et al. [PMW*08] com-

prehensively analysed the problem in the perspective of transformation space and presented a computational model for detecting repeated geometric structures on 3D meshes. Quite a few rewarding papers related to discovering geometric regularity concern the detection of geometric symmetry, a classic and active topic in computer graphics. Latest effort (e.g., [THW*14]) has made it possible to find structural regularities on 3D shapes of widely varying geometry.

The digital equivalent to the peeling stage involves a mesh processing algorithm to enhance the quality of the 3D mesh. In [CGPS08], the authors propose a method to improve the details and fine scale geometry of a 3D mesh in preparation for 3D printing. In addition, producing offsets, such as the proposed by [MHCL15], can enhance the geometry for 3D printing.

In the present work we chose to experiment with additive manufacturing technologies instead of approaching the problem with subtractive technologies, such as CNC. The main reason for this is the increasing availability of AM to amateurs and DIY communities as well as the low prices that are involved in the process. One of the limitations of AM technologies is its limited working volume. Ornamental mouldings are usually larger than the printer area of most 3D printers. Hence, there is a requirement to assemble the fabricated pieces. In recent literature, relevant solutions are presented by [ACP*14,LBRM12,YCL*15] to the assembly of fabricated pieces.

4. Digital Preparation of Ornamental Mouldings

We now describe our proposed method for the automatic segmentation of motifs as well as for the digital restoration of the mouldings in order to digitally take out the layers of painting, a process which is currently handled manually.

4.1. Automatic Motif Segmentation

We observe that the 3D shapes of the mouldings have a quasi-relief structure and the motifs are always of a rectangular shape. Also, the repetition of motifs are caused by translation in one direction. These observed characters significantly ease the problem as the motif can be directly segmented as a cut-off section of the 3D mesh by merely two vertical cutting planes. However, unlike many previous methods, we are not looking for the global geometric regularity, or in mathematical words, the transform T applied over all of the vertices on a mesh M which meets $M = T(M)$. Instead, the targeting motif represents a geometric regularity at some meso-level where in most cases, the macro-level global shape does not matter. It can be seen that for our specific data (many of them have the so called 'egg and dart' pattern and Figure 3 shows two examples), the translational symmetry within the 'egg and dart' pattern may be detected through auto-correlation. However, auto-correlation can only find the translation but neither detect nor segment a single motif since it gives no clue to locate the best cutting planes. We thus developed a method to solve both detection and segmentation of motifs of the 'egg and dart' type. Our main idea is to detect the centres of two adjacent egg and dart units as the anchor points so that we can draw two cutting planes perpendicular to the line connecting them to segment the region (which corresponds to the motif) between them. The workflow of this method is illustrated in Figure 2.

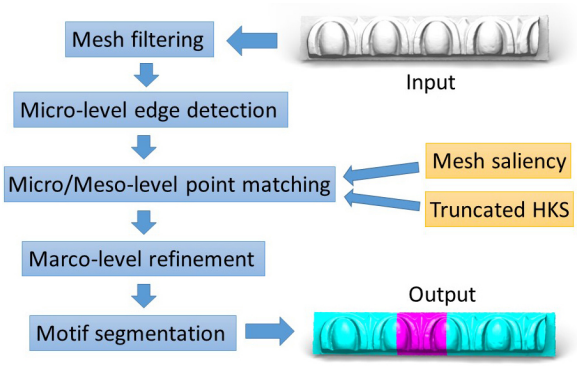

Figure 2: *The work flow of automatic motif extraction*

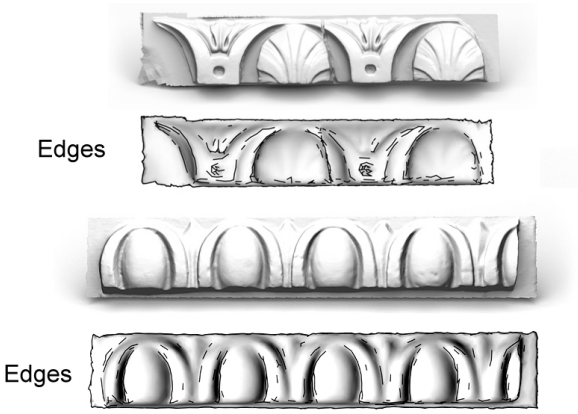

Figure 3: *Micro-level edge detection. Top: edge detection on a shell moulding; Bottom: edge detection on an egg and dart type moulding. Note that the edge detection is implemented on filtered meshes.*

First, we employ Laplacian smoothing to remove noise and some insignificant edges which will be undesired in the next stage of edge detection. Then we implement a simple micro-level edge detection where mesh edges that meet any of the following conditions are detected:

a) The edge is shared by only one triangle.
b) The edge is shared by more than two triangles.
c) The edge is shared by a pair of triangles with angular deviation greater than a threshold. In out work, this threshold is set to $\frac{\pi}{6}$.

Figure 3 shows two examples of edge detection results. The purpose of edge detection is to localise the first anchor vertex (ideally the centre of an egg region) which potentially locate in, or at least is close to one of the cutting planes. Such a coarse localisation can be expressed mathematically as below.

$$m^* = \text{argmax}_{m=1,2,\ldots M} D, \quad D = \text{NN}(E,P) \tag{1}$$

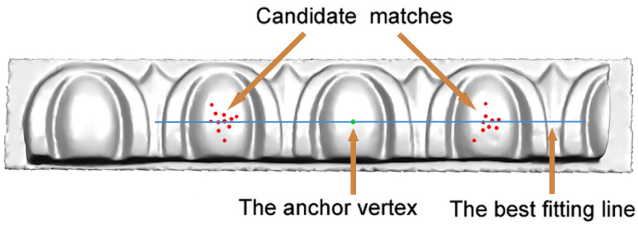

Figure 4: *Macro-level refinement using RANSAC. The RANSAC algorithm is used to find the best fitting line. Then the outliers (the vertices which are not sufficiently close to the line) are removed from the list of candidate matches.*

where $P = \{p_m\}, m = 1,2,...M$ denotes the set of vertices of the input mesh containing M vertices and E is the set of detected edge points. D is M-dimensional vector which stores the distances between a vertex p_m and its closest edge point in E computed by the nearest neighbour algorithm NN. For a moulding mesh displaying the egg and dart pattern, it can be seen that Equation 1 will typically select a vertex p_{m^*} roughly in the centre of the egg region as the anchor vertex since this region is far away from any of the edge vertices.

The next step is to find the matching point of the anchor vertex. This is a classic 3D point matching problem where the prevailing solution is to find the closest point defined by some distance measure in a high dimension space of a certain descriptor. There are a couple of 3D descriptors available in the literature. Here we employ the Kernel Signature (HKS) [SOG09] while some other descriptors might also work. The HKS of a mesh vertex is a function of a parameter t which defines the dimension of the HKS vector. The HKS defined by a small t encodes local or micro-level information of the vertex. When t becomes larger, more meso and macro-level information are embedded into the HKS and the HKS defined by all $t's$ is demonstrated to be highly informative. Motifs only have structural regularity at micro and meso-level while globally they are not symmetric. Thus a pair of matching points which locate at similar positions on two motifs only have similar HKS defined by a small t. In this work, we use a half of the t's to define the HKS to make sure that it only encodes micro and meso-level information around the vertex. However, an HKS truncated by a small t is not so discriminative as one defined by a large t. Therefore, we consider combining other type of information with the HKS for creating a more discriminative descriptor.

Mesh saliency is a measure of regional importance on a surface mesh in accordance with human visual perception. Due to the micro and meso-level geometric similarity between two corresponding vertices, they tend to have similar saliency values. We compute saliency detection using the method proposed in [SLMR14] and extend the HKS vector by adding one extra dimension of saliency.

To further make the matching more reliable, instead of directly finding the closest vertex of the anchor vertex defined by Euclidean distance in the descriptor space, we first find a group of good candidate matching vertices. Usually the number of these candidate matching vertices is between 5% and 8% of the total number of vertices. Then, some macro-level refinement strategies are implemented based on the global positional information of the vertices. First, the correct corresponding vertex of the anchor vertex should be neither quite far away from nor quite close to the anchor vertex since ideally, the distance between them should exactly be the width of one motif. So here we introduce a threshold T_d equal to the distance between the anchor vertex and its closest edge vertex. If for a candidate vertex, its distance to the anchor vertex is smaller than $2.5T_d$ or larger than $6T_d$, it will be removed from the candidate list. Second, as a match to the anchor vertex, it should have an analogous positional property. Due to Equation 1, the anchor vertex is far away to any of the edge vertices. We thus request that the distance between a match vertex and its closest edge vertex is no less than $0.75d_m$ where d_m is the distance between the anchor vertex p_m to its closest edge vertex.

Also, we employed the Random sample consensus (RANSAC) method to further refine the candidate set of matches. As illustrated in Figure. 4, we employed the RANSAC algorithm to find the best fitting line and remove the candidate matches not sufficiently close to it. Firstly, we randomly samples one pair of matches to fix one line. The underlay (or consensus) of this line is defined as the points whose distance to this line are less than some threshold. After many iterations (100 in this work) of this random sampling approach, the final solution is the line that has the largest underlay or the largest 'consensus' and the points within the underlay of this line are the inliers which consist of the consensus. The rest of the points are viewed as outliers and will be removed.

Having implemented these three macro-level refinement, we select from the remaining set of candidate matches the vertex closest to the anchor vertex in the descriptor space in terms of Euclidean distance. This selected vertex is regarded as the best match of the anchor vertex. Then we can draw two cutting planes which are perpendicular to the line linking the anchor vertex and its matching vertex at these two vertices respectively. Figure 5 show some segmentation results of our method.

It is worth mentioning that all the steps of our method can be operated on simplified meshes since we only need to find two vertices to segment the motif. Typically it takes 10 seconds to sort out a mesh containing about 250K and 30 seconds for a mesh with about 500K vertices. However, our method is not reliable for some mouldings containing very complicated motif patterns where in some cases, even human can barely recognise the exact boundaries of motifs. This is because in these cases, usually the simple method we used here for pinpointing the anchor vertex does not work well. To recognise and segment motifs for these mouldings, first we need to manually select the anchor vertex and then the above method can automatically and reliably do the rest of the work.

4.2. Automatic Moulding Enhancement

Traditionally, experts restoring a moulding needed to peel the layers of paint from the mouldings to bring back the original detail. This process is purely manual and the exact degree of peeling in different areas of the moulding is usually hard to control. In this project, we solve this problem in an automatic and controllable manner through the *stochastic Laplacian*. The goal is to extract a multi-resolution mesh basis, and then recompose it while reinforcing some frequencies to achieve multi-scale detail enhancement.

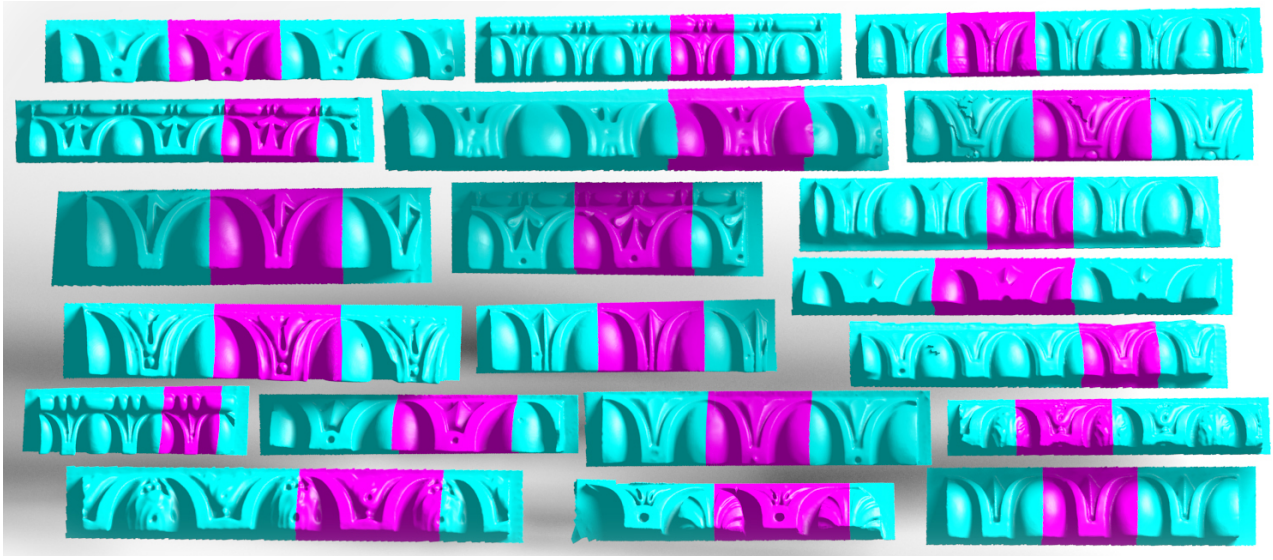

Figure 5: *Rendered results of motif segmentation.*

Given a triangulated mesh M, we first calculate its Laplacian matrix. Typically, the Laplacian matrix of a mesh is based on the discretisation of a continuous Laplacian (e.g., the Laplace-Beltrami operator) defined (mathematically) for a smooth manifold using some weighted sum of adjacent vertices [DRW10]. If a mesh M contains m vertices $p_1,\ldots,p_m$, in its simplest form, the Laplacian matrix can be computed as:

$$L = D - A \tag{2}$$

where A is the adjacency matrix, given by

$$A(i,j) = \begin{cases} 1 & \text{if } p_i \text{ and } p_j \text{ are neighbours} \\ 0 & \text{otherwise} \end{cases}, \tag{3}$$

and D is a diagonal matrix in which D_{ii} is the degree of vertex p_i. This simplest computational model merely takes into account the combinatorics (connectivity). Ideally, a multiscale representation should not only describe the combinatory structure of the mesh, but also encode its local geometric details. To incorporate local small-scale geometric information, the adjacency matrix is weighted by the distances between neighbouring vertices:

$$W(i,j) = \frac{1}{\|p_i - p_j\|^2} A(i,j); \tag{4}$$

This leads to the Laplacian

$$L = D - W. \tag{5}$$

To differ it from the one defined in Eq. (2), we name it *mesh Laplacian*.

We employ Eq. (4) other than the widely used cotangent because we find that it benefits the enhancing of features. The largest angle in an ill-shaped triangle has a negative cotangent but with a large absolute value. Since we need to compute the absolute values of the elements of the Laplacian to transfer it to a stochastic matrix, in the experiments we found that the cotangent Laplacian leads to too much enhancing on ill-shaped triangles. The proposed mesh Laplacian consistent with vertex density is more meaningful since usually most meshes retain more vertices around features (e.g., shape extremities). We also observed that the cotangent Laplacian is not so efficient as the mesh Laplacian.

Algorithm 1: Multiscale representation of mesh

Data: A mesh M containing m vertices represented by a vertex matrix P and a face matrix
Result: A multiscale representation C of the mesh and a basis mesh P_b

begin
  Compute $\widehat{L}$ and then the stochastic Laplacian $\mathcal{L}$, input the maximum number of scales as K; $\mathcal{L}_u = \mathcal{L}$ and $P_{old} = P$;
  for $k \leftarrow 2$ ***to*** K **do**
    $L_u = \arctan(k^{1.5}\mathcal{L}_u\widehat{L}^{j-1})$;
    $\mathcal{L}_u = [L_u]_r$;
    $P_{new} = \mathcal{L}_u P_{old}$;
    $C^{(k-1)} = P_{new} - P_{old}$;
    $P_{old} = P_{new}$;
    if $N_Z/m > 0.1m$ where N_Z is the number of nonzero elements in $\mathcal{L}_u$ **then**
      $P_b = P_{new}$;
      break;
end

In this work, Eq. (5) is followed by two steps. First, we compute $\widehat{L}$ composed of the absolute values of the elements of the mesh Laplacian: $\widehat{L}_{ij} = |L_{ij}|$. Second, we normalise $\widehat{L}$ subsequently so that the sum of each row is 1

$$\mathcal{L} = \left[\widehat{L}\right]_r \tag{6}$$

where $[\cdot]_r$ denotes the row-based normalisation.

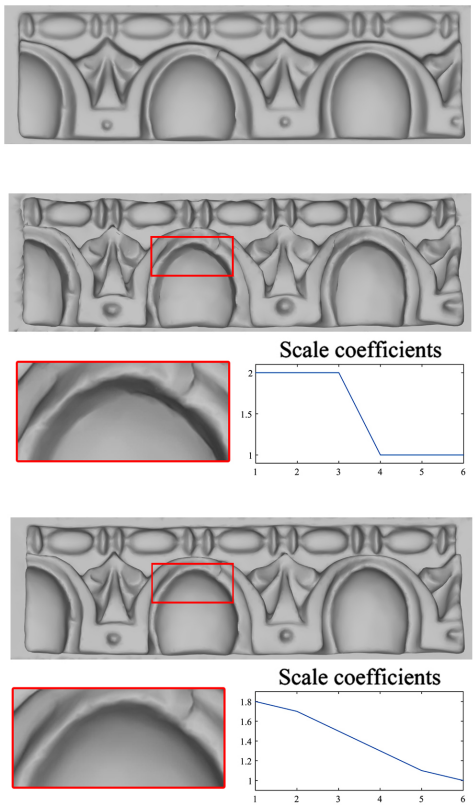

Figure 6: *The effect of scale coefficients. Top row shows the original moulding and the rest are the enhanced ones using different coefficients. It can be seen that scale coefficients make the enhancement controllable and adjustable.*

These two steps are very important since it actually turns the mesh Laplacian to the *stochastic Laplacian*. Here we name it stochastic Laplacian because $\mathcal{L}$ is actually a stochastic matrix and it is inspired by the original Laplacian.

We first explicitly give our algorithm in Algorithm 1. It is based on the iterative updates of the stochastic Laplacian through matrix multiplication, and can be implemented much more easily and efficiently than previous methods which require eigendecomposition of the Laplacian or the design and dilation of wavelets. In the following, we analyse the algorithm and explain why it works.

The row based normalisation $\mathcal{L}_u = [L_u]_r$ in Algorithm 1 guarantees that the vertex matrix is updated by a stochastic matrix in each iteration, which in fact describes the transitions of a Markov chain. It is known that for a stochastic matrix $\mathcal{L}$, $\mathcal{L}_{ij}$ denotes the probability of the one-step transition. Therefore, the k-th stochastic Laplacian produced through a series of $k-1$ matrix multiplications gives the k-step transition probability. Since the matrix of stochastic Laplacian is sparse, most transitions are prohibitive (transition probability equals zero). Only the transitions within a neighbourhood are available because the stochastic Laplacian is constructed based on the adjacency matrix. Hence, the k-step transition actually defines a connected k-ring neighbourhood while all other connectivities/paths are prohibited. When we perform the multiplication $\mathcal{L}_u\widehat{L}^{j-1}$ in Algorithm 1, we essentially perform a displacement in a k-ring neighbourhood for each vertex. The termination condition is that the average neighbourhood contains more than 10% of the mesh vertices since we reasonably assume that this is the maximum size of a single feature (measured by the number of vertices it contains). Such a vertex displacement leads to the loss of local surface details and a hierarchy of meshes with multiple scales of details is formed. The arctan function and the factor $k^{1.5}$ control the degree of such a loss in each iteration. The lost details are stored in the multiscale representation C and we can reconstruct the original mesh through

$$P = P_b + s_1 C^{(1)} + s_2 C^{(2)} + ... + s_{k-1} C^{(k-1)} \tag{7}$$

where $s_1 = s_2 = ... = s_{k-1} = 1$ and we call $\{s_i, i = 1,2,...,k-1\}$ the scale coefficients. As shown in Figure 6 using two different combinations of the scale coefficients results in different enhancement effects although compared to the original moulding, both of them enhance the surface details of the moulding. As a limitation of the work, the selection of the scale coefficients is empirical although some rules are available to follow in the selection process. For example, in Figure 6, it can be seen that a smooth combination of the coefficients leads to a smooth enhancement and a zigzag combination results in non-smooth surface after the enhancement. Usually, the users have to make several trails to find the desired coefficient which can produce the preferred amount of paint peeling. More results of moulding enhancement are shown in Figure 7.

5. Case Study: Restoration of Mouldings in a Household

In order to test the workflow and tools described in the previous sections, we undertook the experimental restoration of a cornice in a room of a house located in a conservation area in the United Kingdom. The proposed workflow offers a cost-effective option to preserve the historical indoor character of the building.

The requirements of the case study were to restore an incomplete cornice which runs throughout the perimeter of the room. Moreover, the area to be restored incorporates a bay window (see Figure 1) requiring for the mouldings to be customised to the shape of the window. Measurements of the room were taken and a CAD model was built with this information as illustrated in Figure 8. In a traditional workflow, it would have been required to peel out the layers of painting of the existing mouldings. However, by using a digital workflow this step was done at a later stage.

The 3D scanning of a selected sample of the existing moulding was conducted using the Breuckmann smartscan device [Bre16] as shown in Figure 9. The areas where existing mouldings were to be completed during the restoration were also scanned. This was done so that a customised joining pieces could be modelled to create seamless joins.

The acquired data was post-processed to reduce noise and fill-in holes in order to produce a 3D mesh of the moulding as shown in Figure 10.

The given cornice exhibits six patterns displaying different types of motifs, including acanthus leafs, flowers as well as egg and darts motifs. The mouldings are made of repeatable *translational motifs*,

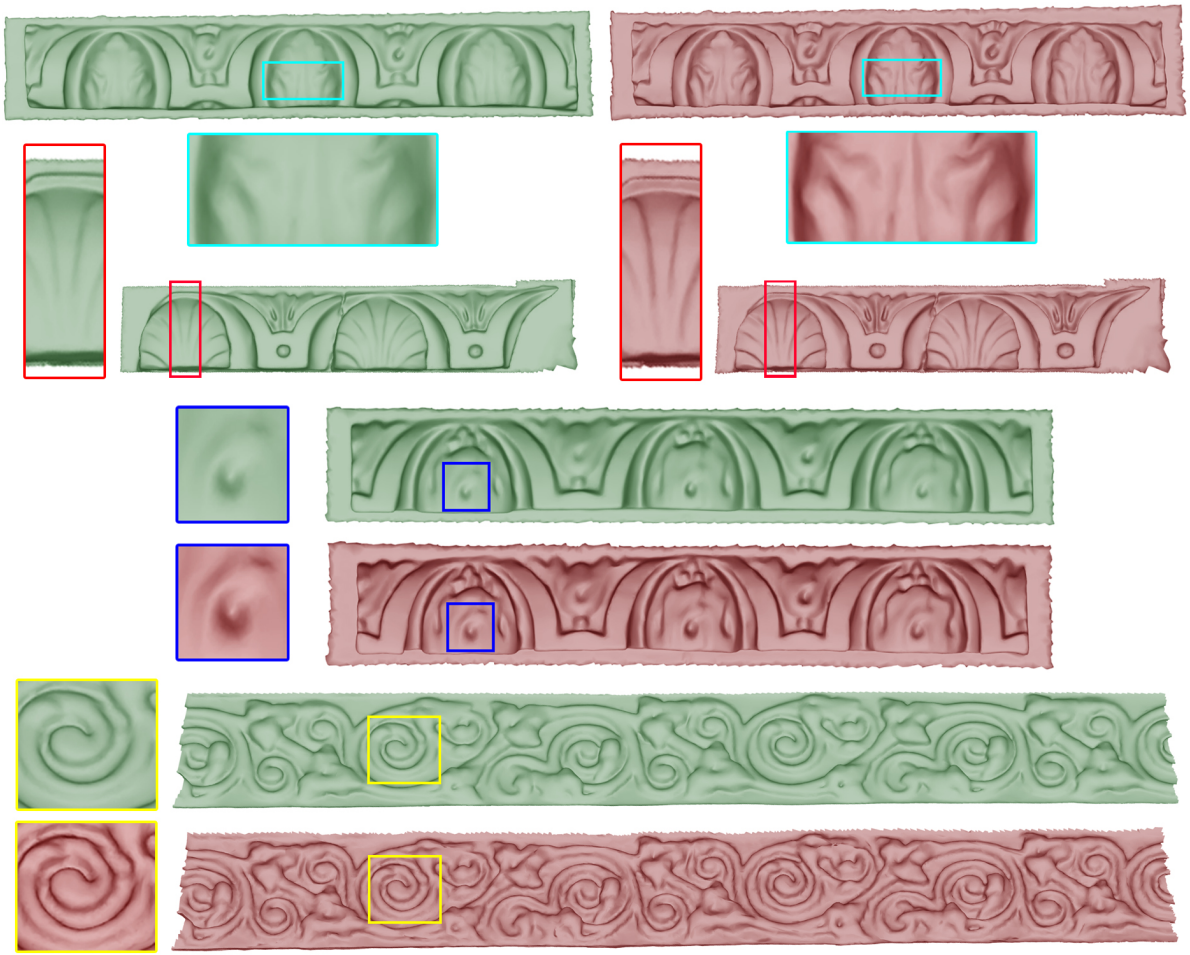

Figure 7: *Results of moulding enhancement. Meshes shaded in green are the original mouldings and the red ones are the enhanced mouldings.*

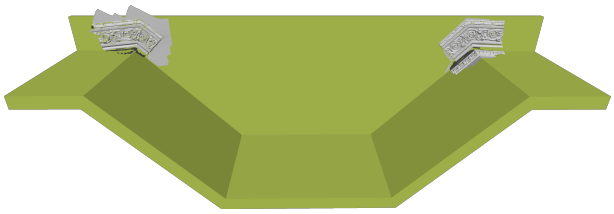

Figure 8: *Area to be restored with the incorporation of ornamental mouldings*

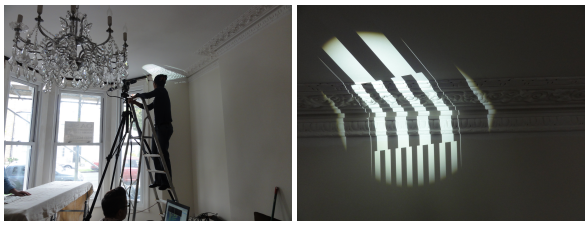

Figure 9: *Digitisation of the cornice for restoration*

thus, their segmentation allowed us to fabricate many to fill-in the perimeter of the area. Our motif segmentation algorithm was only useful for the egg and dart as well as acanthus motifs, as the pattern displaying flowers is of a more challenging type and its segmentation had to be done manually.

For this case study we experimented with two different workflows to incorporate digital fabrication technologies for producing the mouldings:

- Digital Fabrication of Moulds: This incorporates digital fabrication technologies into the traditional workflow by producing a mould using a 3D printed *translational motif*. This approach allowed us to reproduce the ornaments with traditional materials;
- Direct Fabrication of Ornaments: This involved manufacturing directly the ornamental mouldings using AM technologies and post-processing them to achieve a suitable quality.

Figure 10: *Resulting 3D models both of linear and corner pattern containing the different mouldings that need to be fabricated*

The following subsection will describe the experimentation with the proposed workflows.

5.1. Digital Fabrication of Moulds

Currently, two different methods are used to produce the mouldings, running and casting. In this workflow, the first task was to distinguish between the *translational motifs* which are run (profile sections) and those which are casted (periodic repetitions). A total of 8 silicone moulds were required to be produced for the casted parts and 2 running moulds.

For the casting moulds, an automatic detection of the periodic pattern of the mesh was required which has been approached in two steps. The first step was to separate each moulding from the scan using Meshlab [Mes16]. The second step was to detect the periodic *translational motifs*. Then it was required to process the *translational motifs* detected into watertight 3D meshes which could be fabricated.

To produce the watertight 3D mesh we simplified the model to around 5,000 faces. This was done in order to connect the 3D mesh to back and side faces of the printable watertight 3D mesh using Boolean operations. We then replaced the top area by aligning the original higher quality mesh with the simplified mesh and performing a mesh reconstruction algorithm. This process produced a high quality printable 3D mesh as shown in Figure 11.

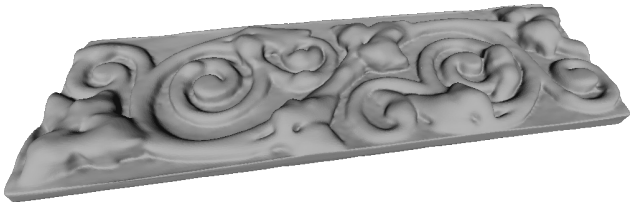

Figure 11: *High quality repeatable translational motif for fabrication to produce cast mouldings*

The incomplete patterns at the edges and the corners were dealt with by using Boolean operations between the scan and the resulting *translational motif* as well as by connecting to *translational motifs at an angle*.

The 8 watertight 3D meshes produced had to be broken into pieces for fabrication since the real scale of the moulds do not fit into our FDM 3D printer working volume. The fabricated workpieces were then pasted together and treated to achieve smoothness. Using these workpieces, a silicone mould was produced by pouring silicone into the printed part which had been encased in a box without a top. By using a traditional method to produce the plaster mouldings, wet plaster was poured on these moulds and plaster *translational motifs* produced.

In addition, for those two profile sections to be produced by a running process, a profile workpiece was digitally produced. This was done using the CGAL library [GW16], which enabled to produce a watertight 3D mesh with the running profile described by the user as a path. For this, we firstly produced a uni-dimensional polygonal path representing the profile based on the 3D scan. Then, the faces were extruded in order to provide thickness to the mould as shown in Figure 12.

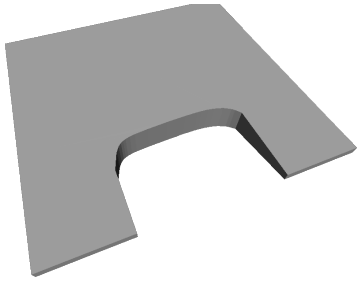

Figure 12: *Mould for running a cornice moulding*

The resulting 3D meshes were fabricated using an FDM 3D printer. These profiles workpieces were also incorporated into the traditional method to produce the plaster mouldings. Hence, wet plaster was produced into a boxed area and the mould was used to run along the plaster to create the profile. We did several iterations of the design as the plaster became easily trapped in the mould as the plastic workpieces do not have the same properties of the zinc profile.

The processes described above worked well enough to produce plaster mouldings in its original material.

5.2. Direct Fabrication of Ornaments

This alternative workflow does not require to distinguish whether a *translational motif* is produced by running or casting as all parts are produced using additive manufacturing technologies. Instead, a *translational motif* was identified for all mouldings and broken into smaller pieces for fabrication.

In total, we require 21 *translational motifs* to deal with all areas which needed to be restored, including the angles of the bay windows and the incomplete shape of the existing mouldings. The *translational motifs* were dealt in a similar way as described in the previous section in order to segment and produce a watertight 3D mesh.

The 21 workpieces were fabricated using an FDM 3D printer. A manual assembly of the sections was required to put the cornice together before fitting it on site (as shown in Figure 13). Figure 1 illustrates the fabricated pieces installed on site and before being glued and painted to cover the joints.

Figure 13: *Assembled section of the cornice fabricated using additive manufacturing technologies*

5.3. Evaluation of the Workflows

After experimenting with both workflows, we evaluated each with regards to expertise required, surface quality, material, time and cost for each workflow.

The digital fabrication of the moulds requires specific expertise to produce the 3D printed workpieces. However, once the silicone moulds are produced, the process requires low expertise to produce the plaster mouldings. The direct fabrication of ornaments requires expertise throughout the workflow to produce the 3D workpieces.

The surface quality produced by the digitally fabricated moulds is the same as for the traditional mouldings as both are produced in plaster. In addition, there are less joining lines as the process is not affected by the size limitations of the AM machine. This is because the *translational motif* can be manufactured in pieces and the part made smoother before producing the mould. On the contrary, in the direct fabrication of ornaments the surface quality is dependent on the AM machine. As such, the surface quality is affected by many joining lines. Although the workpiece could be post-processed to achieve smoothness with the additional time and cost implications.

The plaster material used by the traditional workflow is heavier and more dangerous if not fitted correctly. A positive aspect is that the effects of the plaster material to the room are well understood, and the material is robust and durable. The direct fabrication of ornaments produces a much lighter weight version of the mouldings which is easier to fit by non-experts. However, durability of the resin is not well understood and might decay at a different rate than the rest of the mouldings.

The time and cost of both workflows is an interesting aspect to consider. Both workflows require the same steps in order to produce the workpieces to manufacture. Both share the same digitisation times that were estimated to take 2 days for scanning and post-processing plus 2 days for producing the watertight 3D meshes.

The workflow for the digitally fabrication of the moulds requires less workpieces to be fabricated as the silicone moulds will be used to produce the plaster mouldings. Due to the high customisation required, 10 moulds were required in total to produce the 21 workpieces used to restore the area. We have estimated 6 days to manufacture the 10 workpieces (5 hours for each taking into account an approximate 8-hour working day), 2 days to produce the silicone moulds and 2 days to cast the mouldings in plaster.

In total, this workflow took 13 days to complete. The bottleneck of this process includes the number of printers available as well as the number of silicone moulds. In addition, the cost of material is high as material is required for the FDM printer, for the silicone moulds and for the plaster mouldings. The cost of labour is also high as it includes producing the silicone moulds and casting or running the mouldings.

Alternatively, we calculated the direct fabrication of ornaments took 19 days to complete if only using a single 3D printer. We estimate, 13 days to manufacture the 21 workpieces (5 hours for each taking into account an approximate 8-hour working day) and 2 days to assemble the mouldings. In our case, we had several printers available, thus, this time was considerably reduced. In addition, the cost for material and labour is low in this workflow as only one material is required and the only labour involved after manufacture is assembling the mouldings. This process is more flexible in order to fix problems through iterations in a cost-effective way.

It is difficult to compare these timings to those which will be required by a traditional restoration process. If no master mouldings were available to the experts doing the restoration, building a new master mould will require considerable time and skill. Another approach would have been to take an imprint of the different mouldings on-site. However, a complication of this process is that each *translational motif* will need to be manually segmentated in order to produce separate moulds. Hence, it is estimated that the scanning and post-processing session in both of the proposed workflows could significantly reduce the time and cost of these manual processes.

6. Conclusions and Further work

This paper has presented the definition and testing of a graphical workflow for the fabrication of ornamental mouldings for the restoration of building with historic features. The case study demonstrated how digital fabrication technologies can offer advantages when customisation is required as they can lower the cost of production. Given the fact that there are probably thousands of similar houses in Europe, this research looks promising for people requiring to renovate their properties. The research takes advantages of low-cost tools which are likely to be available to non-expert users in the next decade. Hence, this research can ensure this ornamental decoration does not fall out of use.

Nevertheless, there is still a large area for research. For instance, at the moment the user is required at every stage of the process. Hence, it would be useful to automate the post-processing, segmentation and customisation of the mouldings taking into account the area for restoration. Further work involves achieving this automation as well as improving the algorithms to handle more complex motifs, for example the flower motifs used in the case study which display a more complex segmentation area. More effort is also required to automatically adapt the *translational motifs* into customisable areas such as corners and joins. Finally, more research

is required to improve the production of moulds using digital fabrication technologies, while dealing with the process constraints (e.g. size and material) as well as reducing the time it takes to manufacture the mouldings.

Acknowledgment

The research leading to these results has received funding from the Engineering and the Physical Sciences Research Council (EPSRC) under grant agreement No. EP/L006685/1.

References

[ACP*14] ALEMANNO G., CIGNONI P., PIETRONI N., PONCHIO F., SCOPIGNO R.: Interlocking Pieces for Printing Tangible Cultural Heritage Replicas. In *Eurographics Workshop on Graphics and Cultural Heritage* (2014), Klein R., Santos P., (Eds.), The Eurographics Association. 3

[Bre16] BREUCKMANN: SmartSCAN3D Series, 2016. 6

[CGPS08] CIGNONI P., GOBBETTI E., PINTUS R., SCOPIGNO R.: Color enhancement for rapid prototyping. In *VAST* (2008), Citeseer, pp. 9–16. 3

[CL05] CHITHAM R., LOTH C.: *The classical orders of architecture, 2nd ed.* Architectural, Oxford, 2005. 1

[DRW10] DEY T. K., RANJAN P., WANG Y.: Convergence, stability, and discrete approximation of laplace spectra. In *Proc. ACM-SIAM Symposium on Discrete Algorithms* (2010), pp. 650–663. 5

[GW16] GIEZEMAN G.-J., WESSELINK W.: 2D polygons. In *CGAL User and Reference Manual*, 4.8 ed. CGAL Editorial Board, 2016. 8

[HLL01] HSU J. T., LIU L.-C., LI C.-C.: Determination of structure component in image texture using wavelet analysis. In *Image Processing, 2001. Proceedings. 2001 International Conference on* (2001), vol. 3, IEEE, pp. 166–169. 2

[Jon86] JONES O.: *The Grammar of Ornament*. Studio Editions, London, 1986. 1

[LBRM12] LUO L., BARAN I., RUSINKIEWICZ S., MATUSIK W.: Chopper: Partitioning Models into 3d-Printable Parts. *ACM Transactions on Graphics (Proc. SIGGRAPH Asia) 31*, 6 (Dec. 2012). 3

[LCT04] LIU Y., COLLINS R. T., TSIN Y.: A computational model for periodic pattern perception based on frieze and wallpaper groups. *Pattern Analysis and Machine Intelligence, IEEE Transactions on 26*, 3 (2004), 354–371. 2

[LMLR07] LIU S., MARTIN R. R., LANGBEIN F. C., ROSIN P. L.: Segmenting periodic reliefs on triangle meshes. In *Mathematics of surfaces XII*. Springer, 2007, pp. 290–306. 2

[Mar07] MARSHALL J.: Coded ornament: Contemporary plasterwork and the use of digital technologies. *The Design Journal: An International Journal for All Aspects of Design 10*, 2 (2007). 2

[Mes16] MESHLAB: http://meshlab.sourceforge.net/, 2016. 8

[Mey74] MEYER F. S.: *A Handbook of Ornament*. Duckworth, Trowbridge & Esher, 1974. 1

[MHCL15] MARTINEZ J., HORNUS S., CLAUX F., LEFEBVRE S.: Chained segment offsetting for ray-based solid representations. *Computers & Graphics 46*, 0 (2015), 36 – 47. 3

[PB93] PHILLIPS P., BUNCE G.: *Repeat patterns: a manual for designers, artists and architects*. Thames & Hudson, London, 1993. 1, 2

[PMW*08] PAULY M., MITRA N. J., WALLNER J., POTTMANN H., GUIBAS L. J.: Discovering structural regularity in 3d geometry. In *ACM transactions on graphics (TOG)* (2008), vol. 27, ACM, p. 43. 2

[RES15] RODRIGUEZ-ECHAVARRIA K., SONG R.: Studying Shape Semantics of an Architectural Moulding Collection - Classifying Style Based on Shape Analysis Methods. In *International Congress on Digital Heritage - Theme 3 - Analysis And Interpretation* (2015), Guidi G., Scopigno R., Barceló J., (Eds.), IEEE. 2

[SCP*15] SCOPIGNO R., CIGNONI P., PIETRONI N., CALLIERI M., DELLEPIANE M.: Digital fabrication techniques for cultural heritage: A survey. *Computer Graphics Forum* (2015). 2

[SLMR14] SONG R., LIU Y., MARTIN R. R., ROSIN P. L.: Mesh saliency via spectral processing. *ACM Transactions on Graphics (TOG) 33*, 1 (2014), 6. 4

[SOG09] SUN J., OVSJANIKOV M., GUIBAS L.: A concise and provably informative multi-scale signature based on heat diffusion. In *Proc. SGP* (2009), pp. 1383–1392. 4

[THW*14] TEVS A., HUANG Q., WAND M., SEIDEL H.-P., GUIBAS L.: Relating shapes via geometric symmetries and regularities. *ACM Transactions on Graphics (TOG) 33*, 4 (2014), 119. 3

[TTVG03] TUYTELAARS T., TURINA A., VAN GOOL L.: Noncombinatorial detection of regular repetitions under perspective skew. *Pattern Analysis and Machine Intelligence, IEEE Transactions on 25*, 4 (2003), 418–432. 2

[YCL*15] YAO M., CHEN Z., LUO L., WANG R., WANG H.: Level-Set-Based Partitioning and Packing Optimization of a Printable Model. *ACM Transactions on Graphics (Proc. SIGGRAPH Asia) 34*, 6 (Nov. 2015). 3

[ZJL14] ZHOU S., JIANG C., LEFEBVRE S.: Topology-constrained Synthesis of Vector Patterns. *ACM Trans. Graph. 33*, 6 (Nov. 2014), 215:1–215:11. 2